

SPECTRAL ENERGY DISTRIBUTIONS AND AGE ESTIMATES OF 39 GLOBULAR CLUSTERS IN M31

JUN MA,¹ ZHOU FAN,^{1,2} RICHARD DE GRIJS,^{3,1} ZHENYU WU,¹ XU ZHOU,¹ JIANGHUA WU,¹ ZHAOJI JIANG,¹ AND JIANSHEG CHEN¹
AJ, in press

ABSTRACT

This paper supplements Jiang et al. (2003), who studied 172 M31 globular clusters (GCs) and globular cluster candidates from Battistini et al. (1987) on the basis of integrated photometric measurements in the Beijing-Arizona-Taiwan-Connecticut (BATC) photometric system. Here, we present multicolor photometric CCD data (in the BATC system) for the remaining 39 M31 GCs and candidates. In addition, the ages of 35 GCs are constrained by comparing our accurate photometry with updated theoretical stellar synthesis models. We use photometric measurements from *GALEX* in the far- and near-ultraviolet and 2MASS infrared *JHK_s* data, in combination with optical photometry. Except for two clusters, the ages of the other sample GCs are all older than 1 Gyr. Their age distribution shows that most sample clusters are younger than 6 Gyr, with a peak at ~ 3 Gyr, although the ‘usual’ complement of well-known old GCs (i.e., GCs of similar age as the majority of the Galactic GCs) is present as well.

Subject headings: galaxies: individual (M31) – galaxies: star clusters – galaxies: stellar content

1. INTRODUCTION

The process of galaxy formation and evolution ranks among the most important outstanding problems in astrophysics (e.g., Perrett et al. 2002). One way to better understand the underlying questions is by studying globular clusters (GCs). GCs are often considered the fossils of the galaxy formation process, since they tend to form in the very early stage of their host galaxy’s evolution (Barmby et al. 2000). A GC is a densely packed, gravitationally bound, roughly spherical system of several thousand to about one million stars. They can be observed out to great distances, which implies that they can be used to study and probe the properties of extragalactic systems. The most distant GC systems studied to date are located in the Coma Cluster; their study has been facilitated by *Hubble Space Telescope* (*HST*) Wide Field and Planetary Camera-2 (WFPC2) observations (Baum et al. 1995; Kavelaars et al. 2000; Harris et al. 2000; Woodworth & Harris 2000).

M31 (NGC 224), the Andromeda galaxy, is an early-type spiral galaxy (type Sb), located at a distance of ~ 780 kpc (Staneek & Garnavich 1998; Macri 2001). It is the nearest and largest spiral galaxy in the Local Group of galaxies and has been the subject of many GC studies and surveys. Hubble (1932) first discovered 140 GC candidates characterized by $m_{\text{pg}} \leq 18$ mag. Subsequently, a number of studies (Seyfert & Nassau 1945; Hiltner 1958; Mayall & Eggen 1953; Kron & Mayall 1960) identified ~ 160 GC candidates in M31. Vetešnik (1962) compiled the first major M31 GC catalog, containing about 300 GC candidates and including *UBV* photometric data. The most extensive GC surveys have since been published by Sargent et al. (1977), Crampton et al. (1985), and the Bologna group (Battistini et al. 1980, 1987, 1993). In particular, Crampton et al. (1985) and Battistini et al. (1980, 1987, 1993) provided photometric data in either *UBV* or *UBVR*. These surveys were mostly based on visual searches of photo-

graphic plates and are fairly complete down to $V = 18$ mag ($M_V \sim -6.5$ mag) (Fusi Pecci et al. 1993), although a number of recent studies searched for fainter GCs in M31 (e.g., Mochejska et al. 1998; Barmby & Huchra 2001; Kim et al. 2007). However, Galleti et al. (2006) showed that a significant number of class-D and E GCs with $V \geq 17$ are still to be confirmed (and hence the GC luminosity function is incomplete), and that large surveys are needed to reach a complete sample of M31 GCs. Following on from the first extensive spectroscopic survey of M31 GCs by van den Bergh (1969), a significant number of authors (e.g., Huchra et al. 1982, 1991; Dubath & Grillmair 1997; Federici et al. 1993; Jablonka et al. 1998; Barmby et al. 2000; Perrett et al. 2002; Galleti et al. 2006; Lee et al. 2008, and references therein) embarked on studies of their spatial, kinematic, and metal-abundance properties. The first comprehensive catalog including photometric and spectroscopic data for M31 GCs was assembled by Barmby et al. (2000). The Revised Bologna Catalog (RBC) of M31 GCs was recently published by Galleti et al. (2004) and has since been revised a number of times (Galleti et al. 2005, 2006, 2007). In the primary catalog (Galleti et al. 2004), all known M31 GCs and candidates were compiled based on a literature survey, leading to a total of 1164 entries including 337 confirmed GCs, 688 GC candidates, and 10 objects with undetermined classification. In addition, Galleti et al. (2004) identified 693 known and candidate GCs in M31 using the 2MASS database and included their 2MASS *JHK_s* magnitudes. The latest RBC (V3.5) was updated on March 27, 2008, and includes the newly discovered star clusters from Mackey et al. (2006), Kim et al. (2007), and Huxor et al. (2008). In total, 1567 GCs and GC candidates (509 confirmed GCs and 1058 GC candidates) are known in M31; 421 former GC candidates turned out to be stars, asterisms, galaxies, HII regions, or extended clusters. In addition, the RBC V3.5 includes photometric data of M31 GCs and GC candidates in the far- and near-ultraviolet (FUV and NUV) from the Nearby Galaxies Survey (NGS) of the *Galaxy Evolution Explorer* (*GALEX*) (Rey et al. 2007). Very recently, Caldwell et al. (2009) presented a new catalog of 670 likely star clusters in the field of M31, all with updated high-quality coordinates accurate to $0.2''$, based on images from either the Local Group Survey (Massey 2006) or the Digital Sky Survey.

¹ National Astronomical Observatories, Chinese Academy of Sciences, Beijing, 100012, P. R. China; majun@vega.bac.pku.edu.cn

² Graduate University, Chinese Academy of Sciences, Beijing, 100039, P. R. China

³ Department of Physics & Astronomy, The University of Sheffield, Hicks Building, Hounsfield Road, Sheffield S3 7RH, UK

An accurate and reliable analysis of integrated stellar populations (such as star clusters) is key to understanding the formation and evolutionary process in galaxies. By means of comparisons of integrated populations with models of homogeneous stellar systems, i.e., simple stellar populations (SSPs), recent studies have achieved some success in determining ages and masses for extragalactic star clusters (e.g., de Grijs et al. 2003a,b,c; Bik et al. 2003; Ma et al. 2006; Fan et al. 2006; Ma et al. 2007).

Ma et al. (2006) and Fan et al. (2006) derived age estimates for M31 GCs by fitting SSP models (Bruzual & Charlot 2003, henceforth BC03) to their photometric measurements in a large number of intermediate- and broad-band passbands from the optical to the near-infrared (NIR). For instance, Ma et al. (2007) constrained the age of the M31 GC S312 (B379), using multicolor photometry from the NUV to the NIR, to $9.5^{+1.15}_{-0.99}$ Gyr. S312 (B379) is among the first extragalactic GCs for which the age was estimated accurately using main-sequence photometry, i.e., Brown et al. (2004) estimated its age at $10^{+2.5}_{-1}$ Gyr. This was based on their analysis of the cluster’s color-magnitude diagram (CMD) below the main-sequence turn-off (MSTO) using extremely deep images obtained with the Advanced Camera for Surveys (ACS) on board the *HST*. They performed a quantitative comparison of their resolved stellar photometry with the isochrones of Vandenberg et al. (2006).

In this paper we first describe our new observations and the relevant data-processing steps, as well as the complementary data used from the literature (§2). In §3 we quantitatively compare the spectral energy distributions (SEDs) of the GCs in our sample with the *GALEX* SSP models. Finally, our results and a summary are presented in §4.

2. DATABASE

2.1. The sample

The GC sample used in this paper was taken from the Bologna catalog of Battistini et al. (1987), which contains 827 M31 GCs and GC candidates. In addition, our sample also supplements that of Jiang et al. (2003), who studied 172 GC candidates from Battistini et al. (1987) on the basis of integrated photometric measurements in the Beijing-Arizona-Taiwan-Connecticut (BATC) photometric system. In Jiang et al. (2003), all GC candidates of classes A and B (353 objects) in Battistini et al. (1987) (i.e., their Table IV) were adopted as their original sample. However, of these only 223 objects are in their observed CCD fields. They also noted that B007 is a galaxy, and B055, B132 and B147 are virtually stars (Barmby et al. 2000). These four objects were therefore not included in Jiang et al. (2003)’s final sample. In summary, 219 class-A or B GCs were observed by Jiang et al. (2003), of which 47 were excluded because of missing photometric measurements in some filters. In this paper we analyze these 47 GC candidates on the basis of newly observed data in the BATC photometric system combined with *GALEX* FUV/NUV photometry, broad-band *UBVRI*, and NIR *JHK_s* (2MASS) data. However, we did not manage to obtain accurate photometric measurements for a number of objects because of either the dominance of a nearby very bright object (B095, B176, and B202), the GC candidate being very faint and superimposed on a very high background (B119 and B324), or the GC candidate being located near M32 (B124) or NGC 205 (B331), both also resulting in a very high contribution. In addition, object B330 is faint and located very close to a brighter object, rendering accurate photometry impossible.

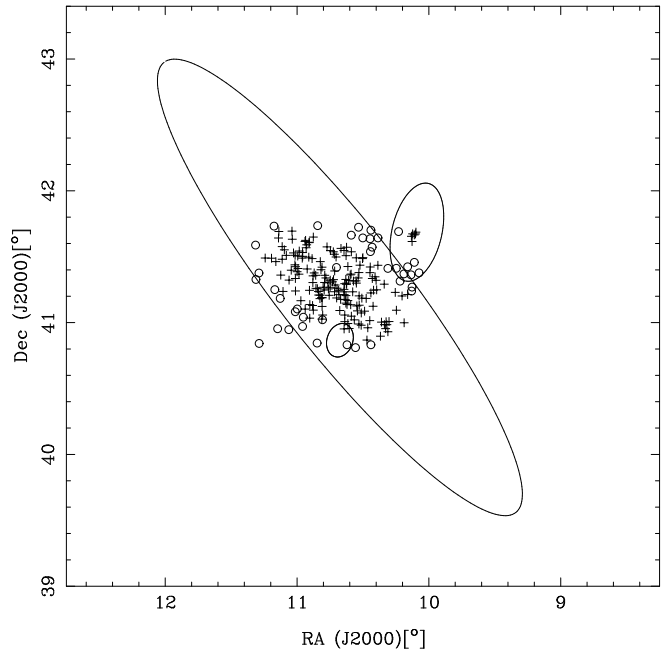


Fig. 1.— Spatial distribution of the GC candidates in M31. Circles and plus signs represent the samples discussed in this paper and by Jiang et al. (2003), respectively. The large ellipse is the M31 disk/halo boundary as defined by Racine (1991); the two small ellipses are the D_{25} isophotes of NGC 205 (northwest) and M32 (southeast).

Thus, here we analyze the multicolor photometric properties of 39 GC candidates. Figure 1 shows the spatial distributions of both our sample GCs (circles) and the Jiang et al. (2003) GCs (plus signs) across the M31 field.

2.2. Observations and data reduction

To obtain photometric measurements in the BATC photometric system for the 39 GC candidates for which Jiang et al. (2003) did not obtain photometry in a number of filters, we re-observed the objects. The BATC photometric system uses a Ford Aerospace 2048×2048 CCD camera with a pixel size of $15 \mu\text{m}$, mounted at the focus of the 0.6/0.9m $f/3$ Schmidt telescope at Xinglong Station (National Astronomical Observatories of China; NAOC). The CCD field of view is $58' \times 58'$, with a pixel size of $1.7''$. The multicolor BATC filter system includes 15 intermediate-band filters covering the wavelength range from 3300\AA to $1 \mu\text{m}$. These filters were specifically designed to avoid contamination from the brightest and most variable night-sky emission lines. The CCD camera is not sensitive at the shortest wavelengths covered by the BATC filters. For this reason, neither Jiang et al. (2003) nor we used the two bluest filters (*a* and *b*) for our observations. Finding charts of the sample GCs and GC candidates in the BATC *g* band (centered at 5795\AA), obtained with the NAOC 60/90cm Schmidt telescope, are shown in Fig. 2.

Thirteen hours of imaging of the M31 field of Jiang et al. (2003) were obtained through the usable set of 13 intermediate-band filters from November 15, 2003 to December 13, 2003. Bias subtraction and flat fielding using dome flats were done with the BATC automatic data-reduction software, PIPELINE 1, originally developed for the BATC Multicolor Sky Survey (Fan et al. 1996; Zheng et al. 1999). The dome flat-field images were taken using a diffuser plate in front of the Schmidt telescope’s corrector plate. This flat-

fielding technique was verified using photometry obtained for other galaxies and spectrophotometric observations (see, e.g., Fan et al. 1996; Zheng et al. 1999; Wu et al. 2002; Yan et al. 2000; Zhou et al. 2001, 2004). Spectrophotometric calibration of the M31 images was done by observations of four F-type subdwarfs, HD 19445, HD 84937, BD +26°2606, and BD +17°4708 (Oke & Gunn 1983). Our magnitudes are therefore defined in the spectrophotometric AB magnitude system (i.e., the Oke & Gunn \tilde{f}_v monochromatic system),

$$m_{\text{BATC}} = -2.5 \log \tilde{F}_v - 48.60, \quad (1)$$

where \tilde{F}_v is the appropriately averaged monochromatic flux in units of $\text{erg s}^{-1} \text{cm}^{-2} \text{Hz}^{-1}$ at the effective wavelength of the specific passband. In the BATC system \tilde{F}_v is defined as (Yan et al. 2000)

$$\tilde{F}_v = \frac{\int d(\log \nu) f_\nu r_\nu}{\int d(\log \nu) r_\nu}, \quad (2)$$

which relates the magnitude to the number of photons detected rather than to the input flux (Fukugita et al. 1996). In Eq. (2), r_ν is the system's response and f_ν the object's SED. Spectrophotometric calibration of the M31 images using the Oke-Gunn standard stars was done during photometric nights (see for details Yan et al. 2000; Zhou et al. 2001). Using these standard-star images, we iteratively obtained atmospheric extinction curves and the variation of these extinction coefficients as a function of the time of night (cf. Yan et al. 2000; Zhou et al. 2001),

$$m_{\text{BATC}} = m_{\text{inst}} + [K + \Delta K(\text{UT})]X + C, \quad (3)$$

where X is the airmass and $[K + \Delta K(\text{UT})]$ the time-dependent extinction term. The instrumental magnitudes (m_{inst}) of selected bright, isolated, and unsaturated stars on the M31 images observed on photometric nights can be readily transformed to the BATC system (m_{BATC}). The calibrated magnitudes of these stars were then used as secondary standards to uniformly combine images from calibrated nights with their counterparts observed on non-photometric nights. Table 1 lists the parameters of the BATC filters and the observational statistics; column 6 provides the scatter, in magnitudes, for the photometric observations of the four primary standard stars in each filter.

2.3. Integrated photometry

For each M31 GC candidate we used the `PHOT` routine in DAOPHOT (Stetson 1987) to obtain the integrated photometry. To avoid contamination from nearby objects, we adopted an aperture of 10.2" diameter, corresponding to 6 pixels. Inner and outer radii for background determination were taken at 8 and 13 pixels from the GC center. Given the small aperture used for the GC observations, aperture corrections were determined as follows. We used isolated stars to determine the magnitude difference between diameter of 6 pixels and the fully integrated magnitude of these stars in each of the 13 BATC filters used. The SEDs for our sample of 39 GCs and GC candidates were then corrected for the filter-specific differences, and these values are given in Table 2. Columns 2–14 give the magnitudes in the 13 BATC passbands used for our observations. For each object the second line lists the 1σ uncertainties in magnitude for the corresponding passband. The errors for each filter are given by DAOPHOT. The magnitudes of B129 in the c and d filters, and that of B195 in p filter could

not be obtained owing to low signal-to-noise ratios in these filters.

2.4. GALEX, broad-band, and 2MASS photometry

To estimate the ages of the M31 sample GCs and GC candidates accurately, we use as many photometric data points covering as wide a wavelength range as possible (cf. de Grijs et al. 2003b; Anders et al. 2004). In addition, Kaviraj et al. (2007) showed that the combination of FUV and NUV photometry with optical observations in the standard broad bands enables one to efficiently break the age-metallicity degeneracy. Worthey (1994) showed that the age-metallicity degeneracy associated with optical broad-band colors is $\Delta \text{age}/\Delta Z \sim 3/2$ (see also MacArthur et al. 2004). However, de Jong (1996) showed that this degeneracy can be partially broken by adding NIR photometry to optical colors, which was recently confirmed by Wu et al. (2005). Cardiel et al. (2003) found that the inclusion of an infrared (IR) passband can improve the predictive power of the stellar population diagnostics by ~ 30 times compared to using optical photometry alone. Since NIR photometry is less sensitive to interstellar extinction than the classical optical passbands, Kissler-Patig et al. (2002) and Puzia et al. (2002) also suggested that it provides useful complementary information that can help to disentangle the age-metallicity degeneracy (also see Galleti et al. 2004).

Rey et al. (2007) published GALEX NUV and FUV photometric data for 485 and 273 M31 GCs, respectively. The photometric data for 28 (NUV) and 17 (FUV) of our M31 sample GCs in common is listed in Table 3. Again, for each object the second line lists the photometric uncertainties for the corresponding passband. The GALEX photometric system is calibrated to match the spectrophotometric AB system.

To date, the study of M31 GCs has been largely based on the excellent Bologna catalog (Battistini et al. 1980, 1987, 1993). Updates to the original RBC were provided by Galleti et al. (2004) who take as their photometric reference the dataset of Barmby et al. (2000) in order to obtain the most homogeneous set of photometric measurements available. Barmby et al. (2000) published optical and IR photometric data for 285 M31 GCs (see their Table 3), obtained with the 4-Shooter CCD mosaic camera and the SAO IR imager on the 1.2m telescope at the Fred Lawrence Whipple Observatory. Photometric measurements in the $UBVRI$ bands were published by Barmby et al. (2000) for most of our sample objects. Therefore, we preferentially adopt the $UBVRI$ measurements of Barmby et al. (2000). For the remaining GCs we follow Galleti et al. (2004), who updated the Bologna catalog with homogenised optical ($UBVRI$) photometry collected from the most recent photometric references available. Galleti et al. (2004) did not include the photometric uncertainties. Although we refer to the original papers, the uncertainties associated with the same object but based on the use of different photometric systems are often very different. In addition, Galleti et al. (2004) transformed their $UBVRI$ photometry to the reference system of Barmby et al. (2000) by applying offsets derived from objects in common between the relevant catalog and the data set of Barmby et al. (2000). The measurements are therefore internally consistent, and referencing the original uncertainties may be irrelevant. Therefore, we only adopted photometric uncertainties as suggested by Galleti et al. (2004), i.e., 0.05 mag in $BVRI$ and 0.08 mag in U . In fact, these photometric uncertainties do not affect our results significantly, as we showed in Fan et al. (2006) (see

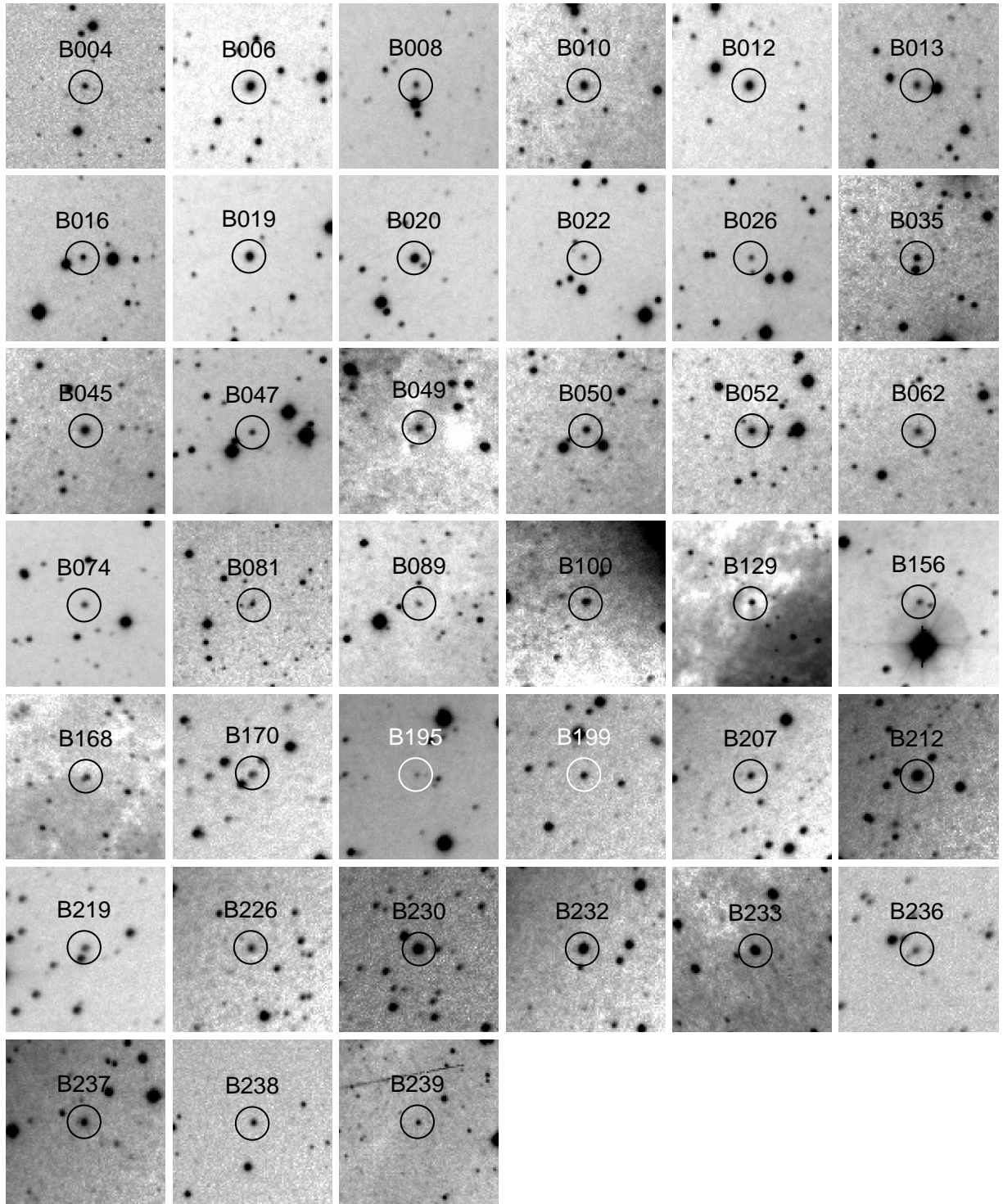


FIG. 2.— Finding charts of the sample GCs and GC candidates in the BATC g band, obtained with the NAOC 60/90cm Schmidt telescope. The field of view of each image is $11' \times 11'$.

their §4.3 for details).

Galleti et al. (2004) identified 693 known and candidate GCs in M31 using the 2MASS database, and determined their 2MASS JHK_s photometric magnitudes (transformed to the CIT photometric system) (Elias et al. 1982, 1983). However, we need the original 2MASS JHK_s magnitudes for our sample GCs to compare our observational SEDs with the SSP models, so we reversed this transformation using the same procedures. Since Galleti et al. (2004) did not provide the 2MASS JHK_s uncertainties, we obtained these by comparing the photometric magnitudes with Fig. 2 of Carpenter et al. (2001). They show the observed photometric rms uncertainties as a function of magnitude for stars brighter than their observational completeness limits. We include the broad-band and 2MASS photometry (and the associated uncertainties) of the sample GCs in Table 3. We also list the new classification flags, following RBC V3.5 notation. From Table 3 we learn that B052 and B062 are classified as galaxies based on their radial velocities. We will therefore not estimate their ages below.

2.5. Comparison with previously published photometry

The BATC intermediate-band system can easily be transformed to the $UBVRI$ broad-band system. Zhou et al. (2003) derived the relationships between these two systems using standard stars from the catalogs of Landolt (1983, 1992) and Galadí-Enríquez et al. (2000):

$$m_B = m_d + 0.2201(m_c - m_e) + 0.1278 \pm 0.076, \quad (4)$$

$$m_V = m_g + 0.3292(m_f - m_h) + 0.0476 \pm 0.027. \quad (5)$$

To check our photometry we derived the magnitudes in B and V based on Eqs. (4) and (5). We transformed the magnitudes of our 39 GCs and GC candidates in the BATC c, d, e bands to B -band photometry, and BATC $f, g,$ and h -band measurements into V -band data. Fig. 3 shows a comparison of our V and $(B - V)$ photometry with previously published measurements of Barmby et al. (2000) and Galleti et al. (2004). The mean V magnitude and $(B - V)$ color differences (in the sense of this paper minus Barmby et al. (2000) or Galleti et al. (2004)) are $\langle \Delta V \rangle = -0.066 \pm 0.013$ mag and $\langle \Delta(B - V) \rangle = -0.040 \pm 0.017$ mag, respectively, thus showing excellent agreement.

2.6. Metallicities and reddening values

To estimate the ages of our sample GCs accurately we required that our GCs have both independently determined metallicities and reddening values. We used three homogeneous sources for spectroscopic metallicities (Huchra et al. 1991; Barmby et al. 2000; Perrett et al. 2002) and one reference (Fan et al. 2008).

Huchra et al. (1991) obtained spectroscopy of 150 M31 GCs and candidates with the Multiple Mirror Telescope (MMT). The system they used has a resolution of 8–9Å and enhanced blue sensitivity. To obtain many of the strongest and most metallicity-sensitive spectral features of interest in the ultraviolet, they extended their observations to the atmospheric cut-off at 3200Å (see details in Brodie & Huchra 1990). The metallicities of these 150 objects were determined using six absorption-line indices from integrated cluster spectra employing the method of Brodie & Huchra (1990).

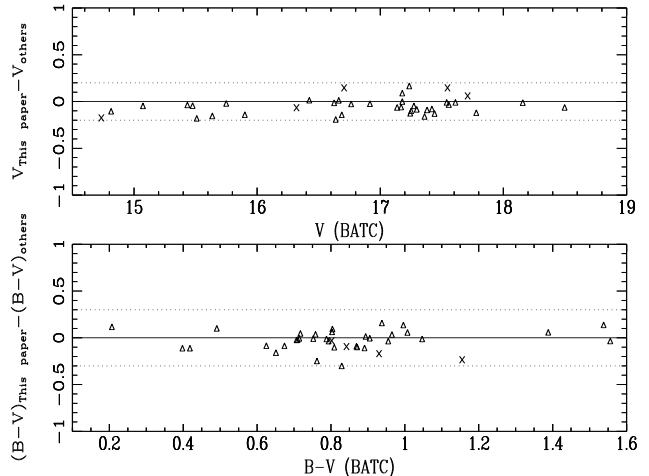


FIG. 3.— Comparison of our newly obtained cluster photometry with previous measurements by Barmby et al. (2000) (triangles) and Galleti et al. (2004) (crosses). The dashed lines enclose ± 0.2 mag in V and ± 0.3 mag in $B - V$.

Barmby et al. (2000) observed 61 M31 GCs and candidates spectroscopically using the Keck Low Resolution Imaging Spectrometer (LRIS) and the MMT Blue Channel spectrograph. With Keck LRIS, they used a $600 \ell \text{ mm}^{-1}$ grating with a $1.2 \text{ \AA pixel}^{-1}$ dispersion from 3670–6200Å, and a resolution of 4–5Å. With the MMT Blue Channel, they used a $300 \ell \text{ mm}^{-1}$ grating with a $3.2 \text{ \AA pixel}^{-1}$ dispersion from 3400–7200 Å, and a resolution of 9–11Å. They obtained the cluster metallicities on the basis of the Brodie & Huchra (1990) method as well.

Perrett et al. (2002) determined metallicities for more than 200 M31 GCs and candidates using the Wide Field Fibre Optic Spectrograph (WYFFOS) at the 4.2m William Herschel Telescope. Their spectral range covers ~ 3700 – 5600 \AA using two gratings, one of which (H2400B, $2400 \ell \text{ mm}^{-1}$) yields a dispersion of $0.8 \text{ \AA pixel}^{-1}$ and a spectral resolution of 2.5 \AA over the range 3700–4500Å, and the other (R1200R, $1200 \ell \text{ mm}^{-1}$) yields a dispersion of $1.5 \text{ \AA pixel}^{-1}$ and a spectral resolution of 5.1 \AA over the range 4400–5600Å. Perrett et al. (2002) calculated 12 absorption-line indices, again using the method of Brodie & Huchra (1990). Through a comparison of the line indices with published M31 GC $[\text{Fe}/\text{H}]$ values from previous studies (Bönoli et al. 1987; Brodie & Huchra 1990; Barmby et al. 2000), they found that the line indices of the CH (G band), Mgb , and Fe53 lines best represented their observed GCs. Therefore, Perrett et al. (2002) determined the metallicities of their sample targets using an unweighted mean of these three $[\text{Fe}/\text{H}]$ values.

Using metallicities from the literature (Huchra et al. 1991; Barmby et al. 2000; Perrett et al. 2002) combined with the RBC, Fan et al. (2008) determined 443 reddening values and intrinsic colors, as well as 209 metallicities for individual clusters without spectroscopic observations.

To use all metallicities as coherently as possible we ranked the sources of M31 GCs metallicities, choosing Perrett et al. (2002) metallicities whenever available because of the large number of metallicity determinations. Metallicities from Barmby et al. (2000) and Huchra et al. (1991) were preferred if Perrett et al. (2002) determinations were not available. If spectroscopic metallicities were missing, we used Fan et al.

(2008). Metallicities were not available for B089 and B226. As a consequence, we do not attempt to determine their ages (see details in §4). The final set of metallicities for the sample clusters is included in Table 4.

For the reddening values of the sample GCs we refer to Barmby et al. (2000) and Fan et al. (2008). Barmby et al. (2000) determined the reddening for each cluster using correlations between optical and IR colors and metallicity, and by defining various ‘reddening-free’ parameters using their large database of multicolor photometry. Barmby et al. (2000) found that the M31 and Galactic GC extinction laws, and the M31 and Galactic GC color-metallicity relations are similar. They estimated the reddening to M31 objects with spectroscopic data using the relationship between intrinsic optical color and metallicity for Galactic clusters. For objects without spectroscopic data they used the relationships between the reddening-free parameters and certain intrinsic colors based on Galactic GC data. Following the methods in Barmby et al. (2000), Fan et al. (2008) (re-)determined reddening values for 443 clusters and cluster candidates. We choose Fan et al. (2008) reddening values whenever available because their reddening values comprise a homogeneous data set and they are larger than those of Barmby et al. (2000). The reddening values for the sample clusters are listed in Table 4. The values of extinction coefficient R_λ are obtained by interpolating the interstellar extinction curve of Cardelli et al. (1989).

3. AGE DETERMINATION

3.1. Stellar populations and synthetic photometry

The most direct method to constrain the ages of different stellar populations involves comparing the observed luminosity levels of the MSTOs. Unfortunately, this approach is limited to the nearest GCs, where individual stars can be resolved and measured down to a few magnitudes fainter than the MSTO. Even in M31, the nearest large spiral galaxy, the MSTO is only reached for one GC (S312) (also see Brown et al. 2004; Rey et al. 2007; Ma et al. 2007). However, since the pioneering work of Tinsley (1968, 1972) and Searle et al. (1973) evolutionary population synthesis modeling has become a powerful tool for the interpretation of integrated spectrophotometric observations of galaxies as well as their components (see e.g. Anders et al. 2004).

In evolutionary synthesis models, SSPs are modeled on the basis of a collection of evolutionary tracks of stars of different initial masses and a set of stellar spectra at different evolutionary stages. To estimate the ages of our sample GCs we compare their SEDs with the GALEV SSP models (e.g., Kurth et al. 1999; Schulz et al. 2002; Anders & Fritze-v. Alvensleben 2003). The GALEV SSPs are based on the Padova isochrones (with the most recent versions using the updated Bertelli et al. (1994) isochrones, which include the thermally-pulsing asymptotic giant-branch [TP-AGB] phase), and a Salpeter (1955) stellar initial mass function with a lower-mass limit of $0.10 M_\odot$ and the upper-mass limit between 50 and $70 M_\odot$, depending on metallicity. The full set of models spans the wavelength range from 91\AA to $160 \mu\text{m}$. These models cover ages from 4×10^6 to 1.6×10^{10} yr, with an age resolution of 4 Myr for ages up to 2.35 Gyr, and 20 Myr for greater ages.

Since our observational data consists of integrated luminosities through a given set of filters, we convolved the theoretical SSP SEDs with the GALEX FUV and NUV, broad-

band *UBVRI*, BATC, and 2MASS *JHK_s* filter response curves to obtain synthetic ultraviolet, optical, and NIR photometry for comparison. The synthetic magnitude in the AB magnitude system for the i^{th} filter can be computed as

$$m_i = -2.5 \log \frac{\int_\lambda F_\lambda \varphi_i(\lambda) d\lambda}{\int_\lambda \varphi_i(\lambda) d\lambda} - 48.60, \quad (6)$$

where F_λ is the theoretical SED and φ_i the response curve of the i^{th} filter of the GALEX FUV/NUV, *UBVRI*, BATC, and 2MASS *JHK_s* photometric systems. Here, F_λ changes as a function of age and metallicity.

3.2. Fitting results

We use a χ^2 minimization test to examine which GALEV SSP models are most compatible with the observed SEDs, following

$$\chi^2 = \sum_{i=1}^{23} \frac{[m_{\lambda_i}^{\text{intr}} - m_{\lambda_i}^{\text{mod}}(t)]^2}{\sigma_i^2}, \quad (7)$$

where $m_{\lambda_i}^{\text{mod}}(t)$ is the integrated magnitude in the i^{th} filter of a theoretical SSP at age t , $m_{\lambda_i}^{\text{intr}}$ represents the intrinsic integrated magnitude in the same filter, and

$$\sigma_i^2 = \sigma_{\text{obs},i}^2 + \sigma_{\text{mod},i}^2. \quad (8)$$

Here, $\sigma_{\text{obs},i}^2$ is the observational uncertainty, and $\sigma_{\text{mod},i}^2$ is the uncertainty associated with the model itself, for the i^{th} filter. Charlot et al. (1996) estimated the uncertainty associated with the term $\sigma_{\text{mod},i}^2$ by comparing the colors obtained from different stellar evolutionary tracks and spectral libraries. Following Wu et al. (2005), Ma et al. (2006), and Fan et al. (2006) we adopt $\sigma_{\text{mod},i}^2 = 0.05$. In fact, the values $\sigma_{\text{mod},i}^2$ adopted do not change the best fits, but only affect the χ^2 values.

The GALEV SSP models include five initial metallicities, $Z = 0.0004, 0.004, 0.008, 0.02$ (solar metallicity), and 0.05. Spectra for other metallicities can be obtained by linear interpolation of the appropriate spectra for any of these metallicities. In addition, if the metallicity of a cluster is poorer than $Z = 0.0004$, we only use the model of $Z = 0.0004$. The best fits to the SEDs of our GCs are presented in Fig. 4.

4. RESULTS AND SUMMARY

In the previous Section we determined the ages of 35 M31 GCs and GC candidates. The results are listed in Table 5. The metallicity of B089 and B226, and the reddening of B089 had not been determined previously. From Fig. 5, which shows the age distribution of the sample clusters (see also Table 5) we conclude that, except for two clusters, the ages of the other sample GCs are all older than 1 Gyr. Most sample GCs are younger than 6 Gyr, with a peak at ~ 3 Gyr. The ‘usual’ complement of well-known old GCs (i.e., GCs of similar age as the majority of the Galactic GCs) is also present.

As discussed in §2.6, to estimate the ages of our sample GCs accurately we required that our GC sample have both independently determined metallicities and reddening values. For metallicity, we used Huchra et al. (1991), Barmby et al. (2000), and Perrett et al. (2002) as our reference data set. Since all of these authors determined the M31 GC metallicities using the calibration of Brodie & Huchra (1990), all three metallicity determinations are on the same [Fe/H] scale and there are no systematic offsets among any of these data

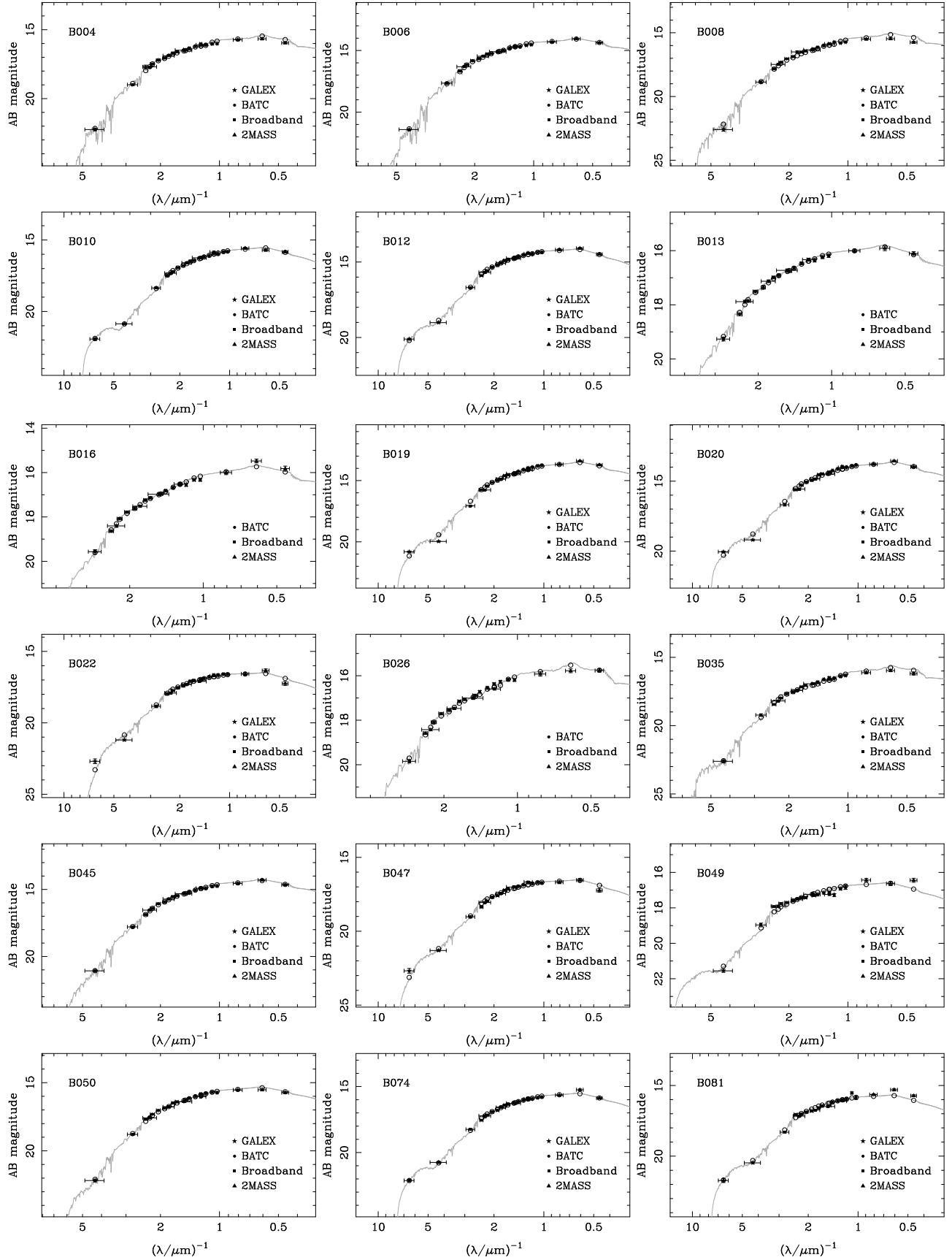


FIG. 4.— Best-fitting integrated SEDs of the GALEX SSP models shown in relation to the intrinsic SEDs for our sample GCs. The photometric data points are represented by the symbols with error bars (vertical error bars for uncertainties and horizontal ones for the approximate wavelength coverage of each filter). Open circles represent the calculated magnitude of the model SEDs for each filter.

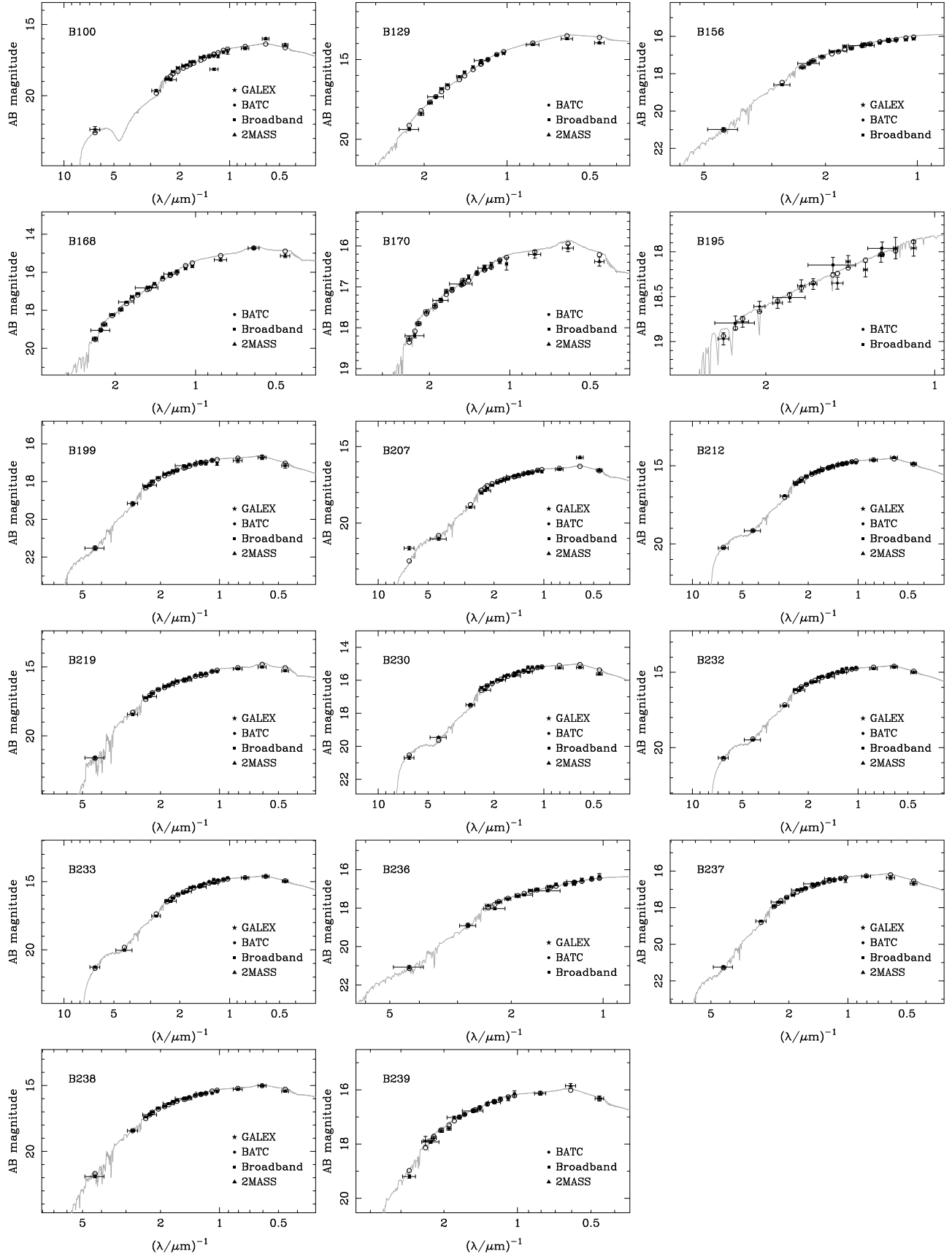


Fig. 4.— Continued.

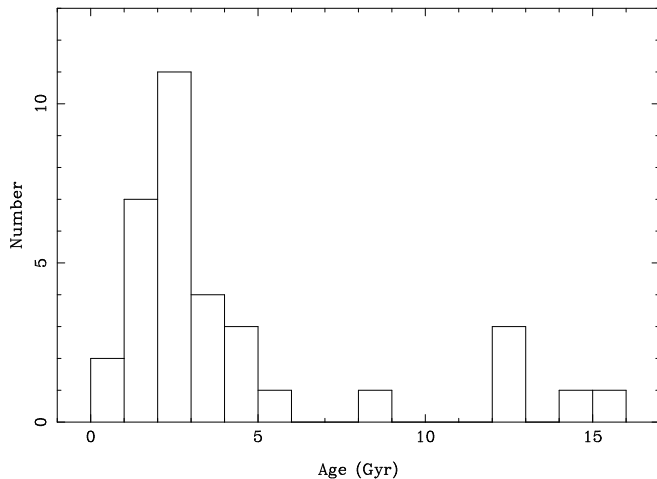


Fig. 5.— Age distribution of our sample GCs and GC candidates in M31.

sets (see details in Perrett et al. 2002). However, individual metallicity differences exist, which may affect our age estimates. Twelve GCs and GC candidates have two metallicity determinations, of which B004, B219, and B238 exhibit the largest differences (> 0.2 dex). The metallicities of B004, B219, and B238 from Perrett et al. (2002) are -0.31 ± 0.74 , -0.01 ± 0.57 , and -0.57 ± 0.66 dex, compared to -1.26 ± 0.59 , -0.53 ± 0.53 , and -1.22 ± 0.76 dex from Huchra et al. (1991). Large metallicity differences lead to large age differences. The ages of B004, B219, and B238 are estimated at 4.10 ± 0.55 , 2.50 ± 0.15 , and 5.00 ± 0.45 Gyr (based on the metallicities of Perrett et al. 2002), compared to 14.40 ± 0.75 , 11.60 ± 1.45 and 14.40 ± 0.80 Gyr (metallicities of Huchra et al. 1991). This implies that the accuracy of the metallicity determinations is very important for the corresponding age estimates. The age differences for the other 10 GCs are less than 1 Gyr based on the metallicities of both Perrett et al. (2002) and Huchra et al. (1991), except for B045: 8.80 ± 1.45 Gyr versus 6.30 ± 0.45 Gyr based on Perrett et al. (2002) and Huchra et al. (1991) metallicities, respectively. In general, the three different sources of spectroscopic metallicities provide homogeneous age estimates. For B004, B219, and B238 the signal-to-noise ratios of the observations of Huchra et al. (1991) and Perrett et al. (2002) are too low. High-quality spectral observations of these three GCs are needed. In addition, we point out that the metallicity calibration of Brodie & Huchra (1990) is solely based on old GCs. However, the sample GCs and GC candidates discussed in this paper are estimated to be young or of intermediate age, so that the age estimates may be somewhat biased by the adopted calibration.

Barmby et al. (2000) discovered that M31 contains GCs exhibiting strong Balmer lines and A-type spectra, from which one infers that these GCs must be very young. Beasley et al. (2004) and Puzia et al. (2005) confirmed this conclusion of Barmby et al. (2000). Burstein et al. (2004) and Fusi Pecci et al. (2005) increased the sample of young M31 GCs to 67. Very recently, Caldwell et al. (2009) determined the ages and reddening values of 140 young clusters in M31 by comparing the observed spectra with model spectra, and these clusters are less than 2 Gyr old. Most have ages between 10^8 and 10^9 yr. The ages of the M31 clusters determined in this paper are in agreement with previous determinations.

Many M31 GCs are resolved in *HST* observations. Some authors, including Ajhar et al. (1996), Fusi Pecci et al. (1996), Rich et al. (1996), Holland et al. (1997), Jablonka et al. (2000), Williams & Hodge (2001a), Williams & Hodge (2001b), and Rich et al. (2005), used WFPC2 images to construct CMDs for determination of the clusters' metallicities, reddening values, and ages. However, these CMDs are usually not deep enough to show conspicuous MSTOs and thus be useful for robust age determinations. In fact, only Williams & Hodge (2001a) and Williams & Hodge (2001b) managed to estimate the ages for four blue massive, compact star clusters and 79 candidate young star clusters by fitting isochrones to the stellar photometry.

Our sample contains four GCs in common with Ajhar et al. (1996) (B006 and B045), Fusi Pecci et al. (1996) (also B006 and B045), and Rich et al. (2005) (B012 and B233). However, only B012 (Rich et al. 2005) could be older than about 8 Gyr (see Gallart et al. 2005), given the presence of a prominent blue horizontal branch, which compares rather poorly with the age obtained here (~ 2 Gyr). However, even with multi-passband photometry spanning from the FUV to K_s , we can only determine cluster ages in a *statistical* sense (also see Gallagher & Grebel 2002; de Grijs et al. 2005).

This discrepancy of a few Gyr highlights the difficulty of obtaining age estimates of unresolved intermediate-age clusters based on multi-passband photometry, given that the color evolution of SSPs is only minimally age dependent once the population has reached an age of $\sim 1 - 3$ Gyr. In addition, although the general age distribution of an entire cluster population (in a given galaxy) can be retrieved fairly self-consistently, the clusters' individual age determinations depend rather strongly on the approach taken to fitting their ages (cf. de Grijs et al. 2005). This, combined with a strong dependence on the adopted reddening and metallicity, results in *individual* age estimates of intermediate-age clusters associated with large uncertainties.

Cluster ages can also be derived by comparing observed with model spectra. Cross-identification of Beasley et al. (2004), Puzia et al. (2005), and Caldwell et al. (2009) with the sample in this paper reveals that only six GCs (and GC candidates) overlap with Puzia et al. (2005) (B006, B012, B045, and B232) and Caldwell et al. (2009) (B049 and B195). The age determinations of two of these (B012 and B232) are inconsistent between Puzia et al. (2005) and this paper: 10.2 ± 2.9 Gyr and 9.0 ± 3.3 Gyr obtained by Puzia et al. (2005) compared to 2.0 ± 0.1 Gyr and 2.0 ± 0.1 Gyr, respectively, obtained in this paper. The ages of the other GCs are consistent among the different determinations.

In fact, the ages of GCs derived by different authors based on a range of methods are not always consistent. For example, the ages of B292 and B327 derived by Beasley et al. (2004) and Puzia et al. (2005) are 2.748 ± 1.151 Gyr and 0.080 ± 0.929 Gyr (Beasley et al. 2004) compared to 9.2 ± 3.3 Gyr and 5.4 ± 1.4 Gyr (Puzia et al. 2005), respectively. On the other hand, Caldwell et al. (2009) estimated the age of B327 at 0.050 Gyr. In addition, the ages of clusters derived in the same paper but based on different line-index measurements are not always consistent either and may indeed differ significantly (see the upper panels of Fig. 5 in Puzia et al. 2005).

ACKNOWLEDGMENTS

We are indebted to the referee for thoughtful comments and insightful suggestions that improved this paper greatly. This study has been supported by the Chinese National Natu-

ral Science Foundation through grants 10873016, 10803007, 10473012, 10573020, 10633020, 10673012, and 10603006,

and by National Basic Research Program of China (973 Program), No. 2007CB815403.

REFERENCES

- Ajhar, E. A., Grillmair, C. J., Lauer, T. R., Baum, W. A., Faber, S. M., Holtzman, J. A., Lynds, C. R., & O'Neil, E. J. 1996, *AJ*, 111, 1110
- Anders, P., & Fritze-v. Alvensleben, U. 2003, *A&A*, 401, 1063
- Anders, P., Bissantz, N., Fritze-v. Alvensleben, U., & de Grijs, R. 2004, *MNRAS*, 347, 196
- Barmby, P., Huchra, J. P., Brodie, J., Forbes, D., Schroder, L., & Grillmair, C. 2000, *AJ*, 119, 727
- Barmby, P., & Huchra, J. P. 2001, *AJ*, 122, 2458
- Battistini, P., Bönoli, F., Braccisi, A., Fusi Pecci, F., Malagnini, M. L., & Marano, B. 1980, *A&AS*, 42, 357
- Battistini, P., Bönoli, F., Braccisi, A., Federici, L., Fusi Pecci, F., Marano, B., & Börngen, F. 1987, *A&AS*, 67, 447
- Battistini, P., Bönoli, F., Casavecchia, M., Ciotti, L., Federici, L., & Fusi Pecci F. 1993, *A&A*, 272, 77
- Baum, W. A., Hammergren, M., Groth, E. J., Ajhar, E. A., & Lauer, T. R., et al. 1995, *AJ*, 110, 2537
- Beasley, M. A., et al. 2004, *AJ*, 128, 1623
- Bertelli, G., Bressan, A., Chiosi, C., Fagotto, F., & Nasi, E. 1994, *A&AS*, 106, 275
- Bik, A., Lamers, H. J. G. L. M., Bastian, N., Panagia, N., & Romaniello, M. 2003, *A&A*, 397, 473
- Bönoli, F., Delpino, F., Federici, L., & Fusi Pecci, F. 1987, *A&A*, 185, 25
- Brodie, J. P., & Huchra, J. P. 1990, *ApJ*, 362, 503
- Brown, T. M., et al. 2004, *ApJ*, 613, L125
- Bruzual, A. G., & Charlot, S. 2003, *MNRAS*, 344, 1000 (BC03)
- Burstein, D., et al. 2004, *ApJ*, 614, 158
- Caldwell, N., Harding, P., Morrison, H., Rose, J. A., Schiavon, R., Kriessler, J. 2009, *AJ*, 137, 94
- Cardelli, J. A., Clayton, G. C., & Mathis, J. S. 1989, *ApJ*, 345, 245
- Cardiel, N., Gorgas, J., Sánchez-Blázquez, P., Cenarro, A. J., Pedraz, S., Bruzual, A. G., & Klement, J. 2003, *A&A*, 409, 511
- Carpenter, J. M., Hillenbrand, L. A., & Skrutskie, M. F. 2001, *AJ*, 121, 3160
- Charlot, S., Worthey, G., & Bressan, A. 1996, *ApJ*, 457, 625
- Crampton, D., Cowley, A. P., Schade, D., & Chayer, P. 1985, *ApJ*, 288, 494
- de Grijs, R., Bastian, N., & Lamers, H. J. G. L. M. 2003a, *MNRAS*, 340, 197
- de Grijs, R., Fritze-v. Alvensleben, U., Anders, P., Gallagher, J. S., Bastian, N., Taylor, V. A., & Windhorst, R. A. 2003b, *MNRAS*, 342, 259
- de Grijs, R., Anders, P., Lynds, R., Bastian, N., Lamers, H. J. G. L. M., & O'Neill, E. J. Jr. 2003c, *MNRAS*, 343, 1285
- de Grijs, R., Anders, P., Lamers, H. J. G. L. M., Bastian, N., Parmentier, G., Sharina, M. E., & Yi, S., 2005, *MNRAS*, 359, 874
- de Jong, R. S. 1996, *A&A*, 313, 377
- Dubath, P., & Grillmair, C. J. 1997, *A&A*, 321, 379
- Elias, J. H., Frogel, J. A., Matthews, K., & Neugebauer, G. 1982, *AJ*, 87, 1029
- Elias, J. H., Frogel, J. A., Hyland, A. R., & Jones, T. J. 1983, *AJ*, 88, 1027
- Fan, X., et al. 1996, *AJ*, 112, 628
- Fan, Z., Ma, J., de Grijs, R., Yang, Y., & Zhou, X. 2006, *MNRAS*, 371, 1648
- Fan, Z., Ma, J., de Grijs, R., & Zhou, X. 2008, *MNRAS*, 385, 1973
- Federici, L., Bonoli, F., Ciotti, L., Fusi Pecci, F., Marano, B., Lipovetsky, V. A., Neizvestny, S. I., & Spassova, N. 1993, *A&A*, 274, 87
- Fukugita, M., et al. 1996, *AJ*, 111, 1748
- Fusi Pecci, F., Cacciari, C., Federici, L., & Pasquali, A. 1993, in: *The Globular Cluster-Galaxy Connection*, eds. G. H. Smith, J. P. Brodie, Vol. 48, p. 410
- Fusi Pecci, F., et al. 1996, *AJ*, 112, 1461
- Fusi Pecci, F., Bellazzini, M., Buzzoni, A., De Simone, E., Federici, L., & Galletti, S. 2005, *AJ*, 130, 554
- Galadř-Enrřquez, D., Trullols, E., & Jordi, C. 2000, *A&AS*, 146, 169
- Gallagher, J. S., & Grebel, E. K. 2002, *IAU Symp.* 207, *Extragalactic Star Clusters*, ed. D. Geisler, E. K. Grebel, & D. Minniti (San Francisco: ASP), 745
- Gallart, C., Zoccali, M., & Aparicio, A. 2005, *ARA&A*, 43, 387
- Galletti, S., Federici, L., Bellazzini, M., Fusi Pecci, F., & Macrina, S. 2004, *A&A*, 426, 917
- Galletti, S., Bellazzini, M., Federici, L., & Fusi Pecci, F. 2005, *A&A*, 436, 535
- Galletti, S., Federici, L., Bellazzini, M., Buzzoni, A., & Fusi Pecci, F. 2006, *A&A*, 456, 985
- Galletti, S., Bellazzini, M., Federici, L., Buzzoni, A., & Fusi Pecci, F. 2007, *A&A*, 471, 127
- Harris, W. E., Kavelaars, J. J., Hanes, D. A., Hesser, J. E., & Pritchett C. J. 2000, *ApJ*, 533, 137
- Hiltner, W. A. 1958, *ApJ*, 128, 9
- Holland, S., Fahlman, G. G., & Richer, H. B. 1997, *AJ*, 114, 1488
- Hubble, E. P. 1932, *ApJ*, 76, 44
- Huchra, J., Stauffer, J., & van Speybroeck, L. 1982, *ApJ*, 259, L57
- Huchra, J. P., Brodie, J. P., & Kent, S. M. 1991, *ApJ*, 370, 495
- Huxor, A. P., Tanvir, N. R., Ferguson, A. M. N., Irwin, M. J., Ibata, R., Bridges, T., & Lewis, G. F. 2008, *MNRAS*, 385, 1989
- Jablonka, P., Bica, E., Bonatto, C., Bridges, T. J., Langlois, M., & Carter, D. 1998, *A&A*, 335, 867
- Jablonka, P., Courbin, F., Meylan, G., Sarajedini, A., Bridges, T. J., & Magain, P. 2000, *A&A*, 359, 131
- Jiang, L., Ma, J., Zhou, X., Chen, J., Wu, H., & Jiang Z. 2003, *AJ*, 125, 727
- Kavelaars, J. J., Harris, W. E., Hanes, D. A., Hesser, J. E., & Pritchett, C. J. 2000, *ApJ*, 533, 125
- Kaviraj, S., Rey, S. C., Rich, R. M., Yoon, S. J., & Yi, S. K. 2007, *MNRAS*, 381, L74
- Kim, S., et al. 2007, *AJ*, 134, 706
- Kissler-Patig, M., Brodie, J. P., & Minniti, D. 2002, *A&A*, 391, 441
- Kron, G. E., & Mayall N. U. 1960, *AJ*, 65, 581
- Kurth, O. M., Fritze-v. Alvensleben, U., & Fricke, K. J. 1999, *A&AS*, 138, 19
- Landolt, A. U. 1983, *AJ*, 88, 439
- Landolt, A. U. 1992, *AJ*, 104, 340
- Lee, M. G., Hwang, H. S., Kim, S. C., Park, H. S., Geisler, D., Sarajedini, A., & Harris, W. E. 2008, *ApJ*, 674, 886
- Ma, J., de Grijs, R., Yang, Y., Zhou, X., Chen, J., Jiang, Z., Wu, Z., & Wu, J. 2006, *MNRAS*, 368, 1443
- Ma, J., et al. 2007, *ApJ*, 659, 359
- MacArthur, L. A., Courteau, S., Bell, E., & Holtzman, J. A. 2004, *ApJS*, 152, 175
- Mackey, A. D., Huxor, A., Ferguson, A. M. N., Tanvir, N. R., Irwin, M., Ibata, R., Bridges, T., Johnson, R. A., & Lewis, G. ApJ, 653, 105
- Mayall, N. U., & Eggen, O. J. 1953, *PASP*, 65, 24
- Macri, L. M. 2001, *ApJ*, 549, 721
- Massey, P., Olsen, K. A. G., Hodge, P. W., Strong, S. B., Jacoby, G. H., Schlingman, W., & Smith, R. C. 2006, *AJ*, 131, 2478
- Mochejska, B. J., Kaluzny, J., Krockenberger, M., Sasselov, D. D., & Stanek, K. Z. 1998, *AcA*, 48, 455
- Oke, J. B., & Gunn J. E. 1983, *ApJ*, 266, 713
- Perrett, K. M., Bridges, T. J., Hanes, D. A., Irwin, M. J., Brodie, J. P., Carter, D., Huchra, J. P., & Watson, F. G. 2002, *AJ*, 123, 2490
- Puzia, T. H., Saglia, R. P., Kissler-Patig, M., Maraston, C., Greggio, L., Renzini, A., & Ortolani, S. 2002, *A&A*, 395, 45
- Puzia, T. H., Perrett, K. M., & Bridges, T. J. 2005, *A&A*, 434, 909
- Racine, R. 1991, *AJ*, 101, 865
- Rey, S. C., et al. 2007, *ApJS*, 173, 643
- Rich, R. M., Mighell, K. J., Freedman, W. L., & Neill, J. D. 1996, *AJ*, 111, 768
- Rich, R. M., Corsi, C. E., Cacciari, C., Federici, L., Fusi Pecci, F., Djorgovski, S. G., & Freedman, W. L. 2005, *AJ*, 129, 2670
- Salpeter, E. E. 1955, *ApJ*, 121, 161
- Sargent, W. L. W., Kowal, C. T., Hartwick, F. D. A., & van den Bergh, S. 1977, *AJ*, 82, 947
- Schulz, J., Fritze-v. Alvensleben, U., Möller, C. S., & Fricke, K. J. 2002, *A&A*, 392, 1
- Searle, L., Sargent, W. L. W., & Bagnuolo, W. G. 1973, *ApJ*, 179, 427
- Seyfert, C. K., & Nassau, J. J. 1945, *ApJ*, 102, 377
- Stanek K. Z., & Garnavich, P. M. 1998, *ApJ*, 503, 131
- Stetson, P. B. 1987, *PASP*, 99, 191
- Tinsley, B. M. 1968, *ApJ*, 151, 547
- Tinsley, B. M. 1972, *ApJ*, 178, 319
- VandenBerg, D. A., Bergbusch, P. A., & Dowler, P. D. 2006, *ApJS*, 162, 375
- van den Bergh, S. 1969, *ApJS*, 19, 145
- Veteřnik, M. 1962, *Bull. Astron. Inst. Czech.*, 13, 182
- Williams, B. F., & Hodge, P. W. 2001a, *ApJ*, 548, 190
- Williams, B. F., & Hodge, P. W. 2001b, *ApJ*, 559, 851
- Woodworth, S. C., & Harris, W. E. 2000, *AJ*, 119, 2699
- Worthey, G. 1994, *ApJS*, 95, 107
- Wu, H., et al. 2002, *AJ*, 123, 1364
- Wu, H., Shao, Z. Y., Mo, H. J., Xia, X. Y., & Deng, Z. G. 2005, *ApJ*, 622, 244
- Yan, H. J., et al. 2000, *PASP*, 112, 691
- Zheng, Z. Y., et al. 1999, *AJ*, 117, 2757

Zhou, X., Jiang, Z. J., Xue, S. J., Wu, H., Ma, J., & Chen, J. S. 2001, ChJAA,
1, 372
Zhou, X., et al. 2003, A&A, 397, 361

Zhou, X., et al. 2004, AJ, 127, 3642

TABLE 1
BATC FILTER PARAMETERS AND OBSERVATIONAL STATISTICS

Filter	λ_{central} (Å)	FWHM (Å)	N^a	Exp. ^b	rms ^c
<i>c</i>	4210	320	3	01:00	0.015
<i>d</i>	4540	340	3	01:00	0.009
<i>e</i>	4925	390	3	01:00	0.015
<i>f</i>	5270	340	3	01:00	0.006
<i>g</i>	5795	310	3	01:00	0.003
<i>h</i>	6075	310	3	01:00	0.003
<i>i</i>	6656	480	3	01:00	0.003
<i>j</i>	7057	300	3	01:00	0.008
<i>k</i>	7546	330	3	01:00	0.004
<i>m</i>	8023	260	3	01:00	0.003
<i>n</i>	8480	180	6	02:00	0.004
<i>o</i>	9182	260	6	02:00	0.003
<i>p</i>	9739	270	6	02:00	0.009

^a Number of exposures for each BATC filter

^b Exposure time (in hr:min)

^c Zero-point error (in mag)

TABLE 2
 BATC INTERMEDIATE-BAND PHOTOMETRY OF OUR SAMPLE OF 39 GCs AND GC CANDIDATES IN M31.

Name	<i>c</i>	<i>d</i>	<i>e</i>	<i>f</i>	<i>g</i>	<i>h</i>	<i>i</i>	<i>j</i>	<i>k</i>	<i>m</i>	<i>n</i>	<i>o</i>	<i>p</i>
B004	17.71	17.49	17.22	17.06	16.72	16.61	16.44	16.34	16.21	16.03	16.09	15.91	16.01
	0.130	0.012	0.008	0.009	0.009	0.008	0.008	0.009	0.010	0.009	0.021	0.010	0.024
B006	16.68	16.17	15.84	15.67	15.29	15.25	15.09	14.98	14.82	14.67	14.70	14.58	14.53
	0.009	0.005	0.004	0.004	0.004	0.004	0.004	0.003	0.004	0.003	0.008	0.005	0.008
B008	17.83	17.33	17.04	16.88	16.51	16.43	16.26	16.14	16.01	15.87	15.73	15.80	15.73
	0.016	0.010	0.007	0.008	0.008	0.007	0.008	0.008	0.009	0.007	0.015	0.011	0.019
B010	17.48	17.21	16.94	16.79	16.50	16.44	16.25	16.17	16.10	15.95	16.00	15.83	15.82
	0.014	0.010	0.007	0.008	0.008	0.007	0.008	0.008	0.011	0.008	0.019	0.012	0.023
B012	15.90	15.58	15.34	15.20	14.91	14.85	14.71	14.63	14.55	14.40	14.45	14.36	14.35
	0.006	0.004	0.003	0.003	0.003	0.003	0.003	0.003	0.004	0.003	0.007	0.004	0.007
B013	18.35	17.86	17.51	17.36	16.99	16.92	16.75	16.64	16.47	16.33	16.36	16.24	16.19
	0.022	0.012	0.009	0.010	0.010	0.010	0.009	0.010	0.012	0.009	0.029	0.015	0.027
B016	18.64	18.08	17.78	17.62	17.24	17.15	16.95	16.82	16.68	16.51	16.56	16.33	16.33
	0.027	0.016	0.011	0.012	0.012	0.011	0.011	0.010	0.014	0.010	0.028	0.016	0.029
B019	15.75	15.45	15.15	14.99	14.61	14.53	14.38	14.25	14.11	13.96	13.89	13.80	13.76
	0.006	0.004	0.003	0.003	0.003	0.003	0.003	0.003	0.003	0.003	0.006	0.004	0.007
B020	15.61	15.29	15.06	14.92	14.54	14.48	14.36	14.24	14.12	13.95	13.99	13.92	13.85
	0.006	0.003	0.003	0.003	0.003	0.003	0.003	0.003	0.003	0.003	0.006	0.004	0.007
B022	17.96	17.74	17.53	17.40	17.09	17.05	16.96	16.89	16.80	16.65	16.65	16.59	16.61
	0.022	0.016	0.013	0.014	0.014	0.013	0.015	0.016	0.022	0.017	0.042	0.028	0.047
B026	18.58	18.09	17.70	17.55	17.15	17.06	16.88	16.72	16.54	16.37	16.27	16.18	16.19
	0.031	0.023	0.016	0.018	0.020	0.015	0.017	0.015	0.018	0.018	0.033	0.022	0.035
B035	18.45	17.98	17.68	17.55	17.17	17.06	16.92	16.81	16.62	16.49	16.52	16.39	16.33
	0.026	0.015	0.011	0.011	0.012	0.011	0.011	0.011	0.013	0.011	0.030	0.018	0.028
B045	16.88	16.41	16.08	15.94	15.55	15.48	15.30	15.19	15.06	14.92	14.93	14.77	14.75
	0.010	0.006	0.004	0.005	0.005	0.004	0.004	0.004	0.005	0.004	0.009	0.007	0.010
B047	18.36	17.95	17.68	17.59	17.23	17.15	17.02	16.96	16.86	16.69	16.77	16.70	16.73
	0.025	0.015	0.011	0.011	0.013	0.011	0.012	0.012	0.016	0.015	0.038	0.023	0.035
B049	17.93	17.76	17.70	17.61	17.43	17.42	17.30	17.25	17.16	17.12	17.28	16.92	17.92
	0.025	0.022	0.020	0.021	0.024	0.019	0.021	0.024	0.026	0.021	0.061	0.040	0.412
B050	17.68	17.32	17.03	16.87	16.49	16.42	16.27	16.14	16.01	15.84	15.78	15.70	15.73
	0.020	0.014	0.011	0.010	0.012	0.010	0.011	0.011	0.013	0.012	0.026	0.017	0.028
B052	19.02	18.24	17.64	17.27	16.92	16.76	16.53	16.38	16.23	16.04	15.89	15.73	15.65
	0.046	0.020	0.012	0.011	0.012	0.010	0.009	0.009	0.012	0.009	0.020	0.013	0.021
B062	18.86	18.17	17.66	17.24	16.96	16.74	16.52	16.44	16.31	16.13	15.98	15.83	15.79
	0.042	0.021	0.014	0.010	0.013	0.010	0.011	0.011	0.014	0.011	0.026	0.016	0.024
B074	17.55	17.16	16.91	16.80	16.43	16.35	16.22	16.14	16.03	15.89	15.92	15.84	15.80
	0.014	0.010	0.007	0.007	0.008	0.007	0.008	0.008	0.009	0.008	0.027	0.013	0.020
B081	17.05	17.01	16.87	16.81	16.59	16.42	16.44	16.18	16.08	16.01	15.95	15.53	15.86
	0.016	0.015	0.013	0.013	0.015	0.014	0.024	0.034	0.032	0.029	0.040	0.049	0.107
B089	18.24	18.22	18.16	18.16	18.11	18.16	18.16	18.16	18.07	18.01	18.49	18.17	18.34
	0.027	0.026	0.026	0.024	0.039	0.034	0.041	0.045	0.050	0.047	0.126	0.090	0.163

TABLE 2
CONTINUED.

Name	<i>c</i>	<i>d</i>	<i>e</i>	<i>f</i>	<i>g</i>	<i>h</i>	<i>i</i>	<i>j</i>	<i>k</i>	<i>m</i>	<i>n</i>	<i>o</i>	<i>p</i>
B100	18.82	18.31	18.04	17.92	17.63	17.61	17.31	17.25	17.24	17.21	17.24	16.95	16.91
	0.050	0.030	0.026	0.026	0.027	0.025	0.026	0.048	0.031	0.033	0.065	0.037	0.170
B129	18.41	17.71	16.83	16.59	16.07	15.79	15.47	15.21	14.99	14.71	14.62
	0.090	0.059	0.034	0.030	0.022	0.019	0.016	0.014	0.014	0.012	0.014
B156	17.67	17.32	17.09	16.82	16.53	16.64	16.44	16.35	16.17	16.20	16.18	16.13	16.40
	0.018	0.011	0.008	0.008	0.008	0.010	0.012	0.014	0.012	0.031	0.021	0.035	0.008
B168	19.50	18.76	18.23	17.96	17.29	17.13	16.78	16.60	16.28	16.07	15.95	15.80	15.69
	0.083	0.053	0.030	0.026	0.025	0.017	0.015	0.015	0.014	0.010	0.027	0.013	0.020
B170	18.27	17.90	17.61	17.46	17.11	17.06	16.84	16.76	16.66	16.52	16.46	16.38	16.44
	0.025	0.020	0.012	0.013	0.014	0.012	0.012	0.014	0.015	0.014	0.033	0.018	0.141
B195	18.97	18.78	18.61	18.57	18.38	18.36	18.35	18.11	18.20	18.04	17.96	17.96	...
	0.046	0.035	0.028	0.035	0.044	0.033	0.044	0.044	0.062	0.059	0.109	0.074	...
B199	18.27	18.00	17.80	17.62	17.44	17.41	17.22	17.10	17.06	17.00	17.05	16.87	17.06
	0.024	0.018	0.012	0.013	0.016	0.013	0.014	0.016	0.018	0.017	0.039	0.022	0.060
B207	18.04	17.74	17.53	17.36	17.14	17.10	16.93	16.84	16.81	16.73	16.71	16.59	16.64
	0.020	0.014	0.011	0.012	0.014	0.013	0.014	0.015	0.020	0.015	0.039	0.023	0.053
B212	16.17	15.91	15.69	15.51	15.31	15.28	15.10	15.01	14.96	14.91	14.84	14.76	14.80
	0.007	0.005	0.004	0.004	0.004	0.004	0.004	0.004	0.005	0.004	0.011	0.006	0.012
B219	17.25	16.90	16.63	16.44	16.15	16.05	15.88	15.76	15.62	15.46	15.46	15.32	15.33
	0.013	0.008	0.006	0.006	0.007	0.006	0.006	0.006	0.007	0.006	0.014	0.008	0.018
B226	19.13	18.51	18.10	17.77	17.55	17.43	17.15	17.05	16.97	16.82	16.63	16.56	16.49
	0.044	0.029	0.015	0.015	0.018	0.015	0.016	0.016	0.022	0.016	0.041	0.021	0.045
B230	16.44	16.33	16.13	15.98	15.75	15.68	15.56	15.47	15.41	15.21	15.21	15.20	15.20
	0.009	0.006	0.005	0.005	0.006	0.005	0.005	0.006	0.007	0.005	0.015	0.008	0.020
B232	16.15	16.02	15.80	15.65	15.34	15.28	15.17	15.06	14.98	14.80	14.74	14.76	14.71
	0.008	0.005	0.004	0.005	0.005	0.005	0.005	0.005	0.006	0.006	0.011	0.008	0.016
B233	16.41	16.19	15.94	15.81	15.44	15.38	15.26	15.15	15.01	14.85	14.85	14.73	14.90
	0.010	0.008	0.007	0.006	0.007	0.006	0.007	0.006	0.008	0.007	0.010	0.015	0.019
B236	17.86	17.69	17.52	17.38	17.08	17.03	16.88	16.75	16.47	16.40	16.45	16.76	16.22
	0.021	0.017	0.012	0.012	0.015	0.012	0.012	0.018	0.023	0.040	0.021	0.039	0.164
B237	17.92	17.70	17.45	17.31	17.01	16.94	16.79	16.70	16.63	16.48	16.50	16.42	16.47
	0.020	0.015	0.012	0.012	0.015	0.013	0.015	0.015	0.016	0.018	0.033	0.024	0.145
B238	17.39	17.02	16.73	16.58	16.23	16.13	15.97	15.88	15.74	15.66	15.58	15.58	15.45
	0.014	0.007	0.006	0.006	0.007	0.012	0.007	0.016	0.016	0.014	0.019	0.011	0.055
B239	17.88	17.79	17.51	17.43	17.01	16.90	16.77	16.66	16.52	16.43	16.33	16.32	16.15
	0.156	0.062	0.040	0.037	0.033	0.025	0.017	0.032	0.032	0.026	0.037	0.063	0.103

TABLE 3
GALEX, BROAD-BAND, AND 2MASS PHOTOMETRY OF THE 39 M31 GCs AND GC CANDIDATES.

Name	c^{\dagger}	FUV	NUV	U	B	V	R	I	J	H	K_s
B004	1	...	22.25	18.29	17.87	16.95	16.36	15.73	14.91	14.36	14.19
		...	0.07	0.03	0.01	0.01	0.02	0.01	0.02	0.07	0.05
B006	1	...	21.41	16.94	16.49	15.53	14.97	14.31	13.48	12.75	12.61
		...	0.04	0.02	0.01	0.01	0.01	0.01	0.03	0.03	0.03
B008	1	...	22.59	18.16	17.66	16.56	16.21	15.51	14.68	14.17	13.98
		...	0.12	0.08	0.05	0.05	0.05	0.05	0.05	0.07	0.06
B010	1	21.93	20.87	17.65	17.50	16.66	16.12	15.48	14.76	14.41	14.07
		0.08	0.03	0.02	0.01	0.01	0.01	0.01	0.03	0.07	0.06
B012	1	20.10	19.02	15.99	15.86	15.13	14.62	14.08	13.36	12.79	12.72
		0.02	0.01	0.01	0.01	0.01	0.01	0.01	0.03	0.03	0.03
B013	1	18.56	18.06	17.19	16.60	15.96	15.18	14.61	14.34
		0.05	0.02	0.01	0.02	0.02	0.03	0.07	0.05
B016	1	18.86	18.58	17.58	16.85	16.15	15.18	14.18	14.05
		0.08	0.04	0.01	0.03	0.02	0.08	0.07	0.10
B019	1	20.81	19.97	16.36	15.94	14.93	14.31	13.74	12.86	12.10	11.96
		0.04	0.02	0.01	0.01	0.01	0.05	0.01	0.02	0.03	0.02
B020	1	20.05	19.20	15.98	15.74	14.91	14.37	13.65	12.97	12.26	12.21
		0.02	0.01	0.08	0.05	0.05	0.05	0.05	0.02	0.03	0.03
B022	1	22.69	21.20	18.14	18.09	17.36	16.97	16.35	15.75	15.04	15.48
		0.16	0.04	0.08	0.02	0.01	0.02	0.02	0.08	0.10	0.12
B026	1	19.14	18.60	17.53	16.88	16.22	15.10	14.48	14.00
		0.06	0.02	0.01	0.03	0.02	0.08	0.07	0.05
B035	1	...	22.61	18.52	18.37	17.48	16.81	16.24	15.30	14.67	14.42
		...	0.10	0.08	0.03	0.01	0.02	0.02	0.08	0.07	0.10
B045	1	...	21.07	17.09	16.72	15.78	15.19	14.54	13.73	13.00	12.89
		...	0.03	0.02	0.01	0.01	0.01	0.01	0.03	0.04	0.03
B047	1	22.68	21.30	18.32	18.23	17.51	16.88	16.30	15.86	15.24	15.47
		0.15	0.04	0.06	0.02	0.01	0.03	0.02	0.08	0.10	0.12
B049	1	...	21.55	18.26	18.08	17.56	17.11	16.87	15.61	15.33	14.68
		...	0.06	0.09	0.04	0.01	0.04	0.04	0.08	0.10	0.10
B050	1	...	22.18	18.09	17.76	16.84	16.27	15.66	14.72	14.22	13.96
		...	0.09	0.05	0.02	0.01	0.02	0.01	0.03	0.07	0.05
B052	4	19.80	18.62	17.21	16.54	15.77	14.70	14.01	13.40
		0.08	0.02	0.01	0.02	0.02	0.04	0.07	0.05
B062	4	19.33	18.58	17.24	16.61	15.82	14.89	14.21	13.66
		0.08	0.02	0.01	0.02	0.01	0.04	0.07	0.05
B074	1	22.12	20.75	17.54	17.40	16.65	16.14	15.58	14.83	13.95	14.11
		0.07	0.02	0.03	0.01	0.01	0.01	0.01	0.02	0.04	0.04
B081	1	21.73	20.47	17.60	17.34	16.80	16.36	15.73	14.82	14.01	13.96
		0.13	0.04	0.02	0.01	0.01	0.02	0.02	0.03	0.07	0.05
B089	2	19.89	19.62	17.96	18.28	18.18	18.22	17.70
		0.03	0.02	0.05	0.04	0.03	0.06	0.06

TABLE 3
CONTINUED.

Name	<i>c</i>	FUV	NUV	<i>U</i>	<i>B</i>	<i>V</i>	<i>R</i>	<i>I</i>	<i>J</i>	<i>H</i>	<i>K_s</i>
B100	1	22.37	...	18.94	19.05	17.91	...	17.77	15.85	14.70	14.67
		0.19	...	0.08	0.07	0.05	...	0.07	0.08	0.07	0.10
B129	1	19.56	17.40	...	14.69	13.25	12.40	12.19
		0.05	0.05	...	0.05	0.03	0.03	0.04
B156	1	...	20.99	17.89	17.63	16.84	16.37	15.87
		...	0.09	0.02	0.02	0.01	0.02	0.05
B168	1	20.82	19.23	17.63	16.69	15.72	14.52	13.43	13.37
		0.08	0.06	0.01	0.03	0.02	0.06	0.04	0.08
B170	1	18.90	18.37	17.39	16.80	16.17	15.38	14.75	14.61
		0.06	0.02	0.01	0.02	0.02	0.08	0.07	0.10
B195	2	19.94	18.97	18.57	18.02	17.59
		0.08	0.06	0.01	0.07	0.05
B199	1	...	21.53	18.45	18.37	17.60	17.03	16.57	16.06	15.42	15.39
		...	0.10	0.08	0.03	0.01	0.03	0.02	0.10	0.10	0.12
B207	1	21.64	21.04	18.26	18.07	17.33	16.81	16.33	15.67	14.42	14.78
		0.11	0.06	0.03	0.02	0.01	0.02	0.02	0.05	0.07	0.08
B212	1	20.27	19.16	16.23	16.22	15.48	15.00	14.48	13.82	13.17	13.11
		0.05	0.02	0.02	0.01	0.01	0.01	0.01	0.03	0.04	0.05
B219	1	...	21.59	17.74	17.32	16.39	15.82	15.19	14.32	13.71	13.51
		...	0.10	0.08	0.05	0.05	0.05	0.05	0.02	0.04	0.04
B226	2	22.09	21.61	19.08	19.04	17.65	...	16.32	15.21	14.47	14.14
		0.14	0.09	0.08	0.05	0.05	...	0.05	0.08	0.07	0.10
B230	1	20.69	19.46	16.78	16.77	16.05	15.61	15.13	14.43	13.92	13.85
		0.08	0.03	0.02	0.01	0.01	0.01	0.01	0.02	0.04	0.05
B232	1	20.67	19.49	16.53	16.38	15.70	15.20	14.65	13.94	13.36	13.25
		0.06	0.02	0.01	0.01	0.01	0.01	0.01	0.03	0.04	0.05
B233	1	21.27	20.04	16.82	16.61	15.80	15.27	14.76	13.90	13.32	13.21
		0.05	0.01	0.01	0.01	0.01	0.01	0.01	0.02	0.04	0.03
B236	1	...	21.07	18.21	18.20	17.38	16.97	16.24
		...	0.07	0.08	0.02	0.01	0.02	0.02
B237	1	...	21.25	18.03	17.87	17.10	16.57	16.05	15.47	15.06	14.91
		...	0.05	0.02	0.02	0.01	0.02	0.02	0.04	0.10	0.09
B238	1	...	21.91	17.73	17.39	16.42	15.86	15.22	14.46	13.72	13.67
		...	0.08	0.02	0.01	0.01	0.01	0.01	0.04	0.04	0.05
B239	1	18.49	18.10	17.08	16.65	16.09	15.31	14.55	14.55
		0.04	0.02	0.01	0.02	0.02	0.04	0.07	0.08

† New classification flag, following RBC V3.5 notation. 1 = confirmed GC, 2 = GC candidate, 4 = confirmed galaxy

TABLE 4
 REDDENING VALUES AND METALLICITIES FOR OUR 39 M31 GCs AND GC CANDIDATES.

Name	$E(B - V)$	ref. ^a	[Fe/H]	ref. ^b
B004	0.07± 0.02	1	-0.31± 0.74	1
B006	0.09± 0.02	1	-0.58± 0.10	1
B008	0.21	2	-0.41± 0.38	1
B010	0.22± 0.01	1	-1.77± 0.14	1
B012	0.12± 0.01	1	-1.65± 0.19	1
B013	0.13± 0.02	1	-1.01± 0.49	1
B016	0.30± 0.02	1	-0.78± 0.19	1
B019	0.20± 0.01	1	-1.09± 0.02	1
B020	0.12± 0.01	1	-1.07± 0.10	3
B022	0.04± 0.03	1	-1.64± 0.07	4
B026	0.15± 0.02	1	0.01± 0.38	1
B035	0.27± 0.05	2	-0.20± 0.54	1
B045	0.18± 0.01	1	-1.05± 0.25	1
B047	0.09± 0.02	1	-1.62± 0.41	1
B049	0.16± 0.02	1	-2.14± 0.55	1
B050	0.24± 0.01	1	-1.42± 0.37	1
B052	0.23± 0.04	1	0.12± 0.17	4
B062	0.26± 0.03	1	-0.47± 0.11	4
B074	0.19± 0.01	1	-1.88± 0.06	1
B081	0.11± 0.02	1	-1.74± 0.40	1
B089
B100	0.48± 0.08	1	-2.21± 0.10	4
B129	1.16± 0.06	1	-1.21± 0.32	1
B156	0.10± 0.02	1	-1.51± 0.38	1
B168	0.54± 0.05	1	-0.12± 0.21	4
B170	0.10± 0.02	1	-0.54± 0.24	1
B195	0.12± 0.00	1	-1.48± 0.63	4
B199	0.10± 0.02	1	-1.59± 0.11	1
B207	0.05± 0.02	2	-0.81± 0.59	1
B212	0.13± 0.01	1	-1.75± 0.13	3
B219	0.05± 0.03	1	-0.01± 0.57	1
B226	1.08± 0.06	1
B230	0.15± 0.01	1	-2.17± 0.16	1
B232	0.14± 0.01	1	-1.83± 0.14	1
B233	0.17± 0.01	1	-1.59± 0.32	3
B236	0.07± 0.05	1	-1.01± 0.17	4
B237	0.14± 0.02	1	-2.09± 0.28	1
B238	0.11± 0.02	1	-0.57± 0.66	1
B239	0.09± 0.01	1	-1.18± 0.61	2

^aThe reddening values are taken from Fan et al. (2008) (ref.=1) and Barmby et al. (2000) (ref.=2).

^bThe metallicities are taken from Perrett et al. (2002) (ref.=1), Barmby et al. (2000) (ref.=2), Huchra et al. (1991) (ref.=3), and Fan et al. (2008) (ref.=4).

TABLE 5
AGES ESTIMATES FOR 35 GCs AND GC CANDIDATES IN M31.

Name	Age (Gyr)	χ^2_{\min} (per degree of freedom)	Name	Age (Gyr)	χ^2_{\min} (per degree of freedom)
B004	4.10 ± 0.55	3.13	B100	0.50 ± 0.10	14.38
B006	12.50 ± 0.65	1.39	B129	15.10 ± 0.70	9.00
B008	2.00 ± 0.10	6.54	B156	4.90 ± 0.65	2.09
B010	1.80 ± 0.10	1.08	B168	12.60 ± 0.20	3.27
B012	2.00 ± 0.10	1.54	B170	4.00 ± 0.45	1.39
B013	12.00 ± 2.00	0.96	B195	0.70 ± 0.15	0.82
B016	2.40 ± 0.30	1.95	B199	3.30 ± 0.55	1.38
B019	2.10 ± 0.10	12.01	B207	1.20 ± 0.10	7.99
B020	1.80 ± 0.10	7.50	B212	1.80 ± 0.10	0.75
B022	3.40 ± 0.15	4.11	B219	2.50 ± 0.15	3.06
B026	3.50 ± 0.25	3.28	B230	1.60 ± 0.10	4.59
B035	1.00 ± 0.10	3.97	B232	2.00 ± 0.10	2.62
B045	8.80 ± 1.45	0.78	B233	2.30 ± 0.10	3.73
B047	2.80 ± 0.20	4.22	B236	2.00 ± 0.25	2.63
B049	1.60 ± 0.10	7.82	B237	3.50 ± 0.35	1.41
B050	16.00 ± 0.30	2.12	B238	5.00 ± 0.45	2.01
B074	2.10 ± 0.15	2.12	B239	14.50 ± 2.05	1.70
B081	2.10 ± 0.20	7.82			